Topological Bogoliubov Quasiparticles from Bose-Einstein Condensate in a Flat Band System

Zahra Jalali-mola [1], Tobias Grass [2,3,1], Valentin Kasper [1,4], Maciej Lewenstein [1,5] and Utso Bhattacharya [1]

[1]*ICFO—Institut de Ciencies Fotoniques, The Barcelona Institute of Science and Technology, 08860 Castelldefels, Barcelona, Spain*
[2]*DIPC—Donostia International Physics Center, Paseo Manuel de Lardizábal 4, 20018 San Sebastián, Spain*
[3]*Ikerbasque—Basque Foundation for Science, Maria Diaz de Haro 3, 48013 Bilbao, Spain*
[4]*Nord Quantique, 3000 boulevard de l'Université (P1-ACET), Sherbrooke J1K 0A5, Quebec, Canada*
[5]*ICREA, Passeig de Lluís Companys 23, 08010 Barcelona, Spain*

For bosons with flat energy dispersion, condensation can occur in different symmetry sectors. Here, we consider bosons in a kagome lattice with π-flux hopping, which, in the presence of mean-field interactions, exhibit degenerate condensates in the Γ and the K point. We analyze the excitation above both condensates and find strikingly different properties: For the K-point condensate, the Bogoliubov–de Gennes (BdG) Hamiltonian has broken particle-hole symmetry and exhibits a topologically trivial quasiparticle band structure. However, band flatness plays a key role in breaking the time-reversal symmetry of the BdG Hamiltonian for a Γ-point condensate. Consequently, its quasiparticle band structure exhibits nontrivial topology, characterized by nonzero Chern numbers and by the presence of edge states. Although quantum fluctuations energetically favor the K-point condensate, the interesting properties of the Γ-point condensate become relevant for anisotropic hopping. The topological properties of the Γ-point condensate get even richer in the presence of extended Bose-Hubbard interactions. We find a topological phase transition into a topological condensate characterized by high Chern number and also comment on the realization and detection of such excitations.

Introduction.—The discovery of topological band structures has led to an entire new field of physics on topological properties of quantum matter [1,2]. The nontrivial topology of bulk Bloch bands in topological insulators and superconductors possesses gapless edge states which are robust against local impurities and give rise to responses that are precisely quantized. A prototypical example of a topological insulator is a fermionic two-dimensional integer quantum Hall system [3], which exhibits a quantized Hall conductivity proportional to the nonzero Chern number of the occupied bands. The nonzero value of the Chern number originates from the breaking of time-reversal symmetry (TRS) due to an applied magnetic field and is responsible for the existence of unidirectional gapless chiral modes propagating along the edges of the system; however, the bulk is completely insulating. In the presence of interactions, such systems may develop topological order, with even more striking phenomena such as anyonic quasiparticles [4], possibly even for mean-field interactions as in the case of Majorana modes in a p-wave superconductor.

However, the notion of topological protection is not tied to fermionic systems only, as interactions also open an avenue for probing topological band structure in bosonic systems, as observed in beautiful quantum gas experiments with cold bosonic atoms [5,6]. While in such a case the nontrivial topology is already present on the level of the single-particle band structure and interactions are only a tool to fill the topological band with bosonic particles, there are other scenarios in which the topologically nontrivial behavior is induced only by the interactions. In particular, bosonic condensates with broken TRS can give rise to collective excitations which exhibit topological bands [7,8]. This exotic phenomenon may happen in degenerate bands and has recently been observed by preparing a Bose-Einstein condensate (BEC) within the p band of a honeycomb lattice [9].

An extreme case of band degeneracy is a flat band where many single-particle states are dispersionless and localized. Quantum systems with a flat energy dispersion have recently attracted a lot of attention, especially due to the realization of flat bands in magic-angle twisted bilayer graphene [10], as well as in synthetic systems [11–16]. While electronic flat band systems have attracted a lot of attention due to unconventional superconductivity in synthetic systems, the important question of bosonic condensation in the presence of vanishing of kinetic energy can be studied. Lifting of the flatness through mean-field interactions as well as the quantum geometry of Bloch states have been discussed as mechanisms which, out of many degenerate states, favor a stable BEC. This turns the mean-field ansatz into a self-consistent description. Still, the flat
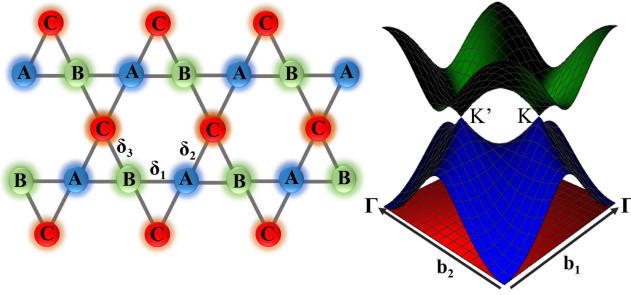
FIG. 1. Kagome lattice with three different sublattices in the left panel and single-particle dispersion relation of the tight-binding Hamiltonian in Eq. (1) for $t > 0$ in the right panel. Here, δ_i represents the distance between two different nearest-neighbor sublattices, and b_i stands for the reciprocal lattice vectors in momentum space.

band scenario comes with some caveats: The huge single-particle degeneracy of the band may survive on the mean-field level and may be resolved only by the contribution of fluctuations through a mechanism known as order by disorder [17,18]. For instance, a mean-field BEC can select the Γ point or the K point, as well as an extensive number of configurations with broken translational symmetry, but the degeneracy is lifted through quantum and/or thermal fluctuations. As shown in Ref. [12], in the limit of very low temperature the K-point condensate is selected, whereas thermal fluctuations might lead to condensates with broken translational symmetry.

Optical lattices with kagome geometries [19,20] and their topological properties [21–24] have come under scrutiny in recent years. Condensation in the flat band is possible via artificial gauge fields, making it the energetically lowest band. Schemes to produce such gauge fields have been developed for a variety of synthetic quantum systems [25–32]. In this Letter, we consider the scenario of a kagome lattice with a synthetic π flux. As shown in Fig. 1, the lowest band of this system is the flat one. We then see that, out of this degenerate manifold, the presence of on-site and nearest-neighbor interactions selects two possible translationally invariant mean-field condensates, at the Γ point and at the K point. Then the collective excitations above these condensates on the level of a quadratic Bogoliubov–de Gennes (BdG) Hamiltonian are studied. We summarize the two key findings from our analysis at the outset: (a) We show that the symmetry properties of the BdG Hamiltonian depend crucially on the wave vector of the condensate. Strikingly, although the single-particle bands are topologically trivial, band flatness and on-site interactions conspire to render the condensate at the Γ point nontrivial. This condensate may further undergo a topological phase transition into bands with higher Chern number through the presence of nearest-neighbor interactions [33]. (b) While the nontrivial condensate is unstable with respect to the zero-point fluctuations in the case of a

kagome lattice with isotropic hopping, we explicitly argue how one can overcome this challenge by engineering anisotropic hopping terms which can enforce the topological condensate [34], with possible scope for experimental realization with an ultracold artificial kagome lattice. In Supplemental Material [35], we provide exact numerical checks via diagonalization and density matrix renormalization group, demonstrating the stability of the BEC.

System.—The kagome structure is composed of three sublattices A, B, and C (the left panel in Fig. 1), and the tight-binding Hamiltonian of particles on such a lattice is $H_0 = t \sum_{\langle i,j \rangle \atop \alpha,\beta} d_{i,\alpha}^\dagger d_{j,\beta} - \mu \sum_{i,\alpha} d_{i,\alpha}^\dagger d_{i,\alpha}$, where $d_{i,\alpha}$ ($d_{i,\alpha}^\dagger$) is the annihilation (creation) operator for particles on sublattice α located at position i. The amplitude of hopping between nearest neighbors $\langle i, j \rangle$ is $t > 0$, and the π flux is accounted by the sign of the hopping term. In momentum space, the Hamiltonian reads

$$H_0(k) = \begin{bmatrix} -\mu & 2t \cos k_1 & 2t \cos k_2 \\ 2t \cos k_1 & -\mu & 2t \cos k_3 \\ 2t \cos k_2 & 2t \cos k_3 & -\mu \end{bmatrix}, \quad (1)$$

with $k_i = \mathbf{k} \cdot \boldsymbol{\delta}_i$ where $\boldsymbol{\delta}_i$ is the vector between two nearest neighbors, as defined in the left panel in Fig. 1. In the rhomboidal Brillouin zone (right panel in Fig. 1), we observe a band touching at $\Gamma = (0,0)$ between the flat band and the middle band and between the middle band and the upper band at the K and K' points. For the interactions, we consider repulsive on-site interactions U and also account for possible nearest-neighbor interactions V in the interaction Hamiltonian given by $H_I = (U/2) \sum_{i,\alpha} (n_{i,\alpha} n_{i,\alpha} - 1) + (V/2) \sum_{\langle i,j \rangle \atop \alpha,\beta} n_{i,\alpha} n_{j,\beta}$, where the density operator is $n_{i,\alpha} = d_{i,\alpha}^\dagger d_{i,\alpha}$.

In a mean-field treatment, the bosonic operators are replaced by their expectation values, $\langle d_k \rangle = d_k^\circ = (\psi_{k,A}, e^{i\phi_{k,B}}\psi_{k,B}, e^{i\phi_{k,C}}\psi_{k,C})$, which are found by minimizing the energy. We concentrate on translationally invariant mean-field solutions in which condensation occurs in a single mode, denoted k_{cp}. We use the hopping parameter t as a unit of energy, and the chemical potential μ serves to adjust the condensate density $\rho = \sum_\alpha |\Psi_{k_{cp},\alpha}|^2$, which we set to 1. The interaction parameters U and V are considered tunable, and we find that qualitatively two regimes must be distinguished. (i) $U > 2V$.—In this physically easily realizable scenario, the mean-field energy $E_{Min} = -2t\rho + (U + 4V)\rho^2/3$ occurs in two modes, at the Γ and K points. In both modes, the mean-field solution is uniform in the sublattices, i.e., $|\psi_\alpha|^2 = \rho/3$. An important difference between the two degenerate condensates is the complex phase in the Γ-point condensate, in contrast to the K-point. Specifically, the two solutions read

$$d_\Gamma^\circ = \frac{1}{\sqrt{3}}(1, -e^{i\pi/3}, e^{2i\pi/3}), \qquad d_K^\circ = \frac{1}{\sqrt{3}}(1, 1, -1). \quad (2)$$

(ii) $U < 2V$.—In this case, the energy is minimal only at the Γ point. As a result of strong nearest-neighbor interaction, the condensate is not uniform in the sublattice anymore. In addition, we mention that at $U = 2V$ the infinite degeneracy of the flat band, which is typically removed by the interactions, reappears as a consequence of the competition between U and V. However, further investigations in this direction are beyond the scope of this Letter.

Bogoliubov quasiparticles.—Despite the possibly very interesting physics which may occur for dominant V, in the following, we focus on the more physical scenario (i). To account for quantum fluctuations around the mean field and obtain the excitations of the mean-field system, we split the operators into mean-field part and fluctuations, $d_k = d_{k_{cp}}^\circ + \delta d_k$, where $\delta d_k = (1 - \delta_{k,k_{cp}})d_k$ is zero at the condensation point. To obtain a quadratic BdG Hamiltonian, $H_B(k) = \frac{1}{2}\sum_{\alpha,\beta}\Psi_{k,\alpha}^\dagger H_{\alpha,\beta}^{MF}\Psi_{k,\beta} + \text{const}$, we keep fluctuating terms only to second order and define Nambu spinors $\boldsymbol{\Psi}_k = (\Psi_{k_+}, \Psi_{k_-}^\dagger)^T$, in which the two components represent particlelike and holelike parts of the wave function, with $\Psi_{k_\pm} = (\delta d_{k_\pm,A}, \delta d_{k_\pm,B}, \delta d_{k_\pm,C})^T$ and $k_\pm = k_{cp} \pm k$. The kernel of the BdG Hamiltonian reads

$$H_B = \begin{bmatrix} H_0(k_{cp} + k) + \mathcal{H}_0(k) & H_\Delta(k) \\ H_\Delta^*(k) & H_0^T(k_{cp} - k) + \mathcal{H}_0^*(k) \end{bmatrix}, \quad (3)$$

where the diagonal part contains the tight-binding Hamiltonian $H_0(k)$ from Eq. (1) and a mean-field contribution $\mathcal{H}_0(k)$ from the interactions. The off-diagonal terms H_Δ stem exclusively from the mean-field decomposition of interactions; see Supplemental Material [35] for explicit expressions.

Diagonalization of the BdG Hamiltonian needs to account for the commutation relation of the Nambu spinors [42], $[\Psi_k, \Psi_{k'}^\dagger] = \sigma_3\delta_{k,k'}$, where $\sigma_3 = \sigma_z \otimes I_3$ acts on Nambu space as the Pauli matrix σ_z. The eigenmodes of the BdG Hamiltonian are obtained from the pseudo-Hermitian Hamiltonian $\sigma_3 H_B(k)$, and the transformation matrix $W(k)$ which diagonalizes $\sigma_3 H_B(k)$ satisfies the following relations:

$$W^\dagger(k)\sigma_3 W(k) = \sigma_3, \quad (4)$$

$$W^\dagger(k)H^{MF}(k)W(k) = \text{diag}[\boldsymbol{\omega}(k_+), \boldsymbol{\omega}(k_-)], \quad (5)$$

$$W^{-1}\sigma_3 H^{MF}(k)W(k) = \sigma_3\text{diag}[\boldsymbol{\omega}(k_+), ..., \boldsymbol{\omega}(k_-)]. \quad (6)$$
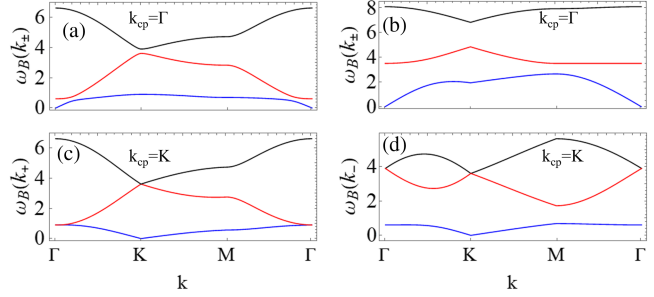

FIG. 2. Bogoliubov dispersions of quasiparticle and quasiholes, for different values of nearest-neighbor interaction V and fixed on-site interaction $U/t = 3$. The value of nearest-neighbor interaction is $V/t = 0.5$ in panels (a)–(d) and $V/t = 4$ in panel (b). In panels (a) and (b), condensation occurs at $k_{cp} = \Gamma$. In this case, particle-hole symmetry leads to $\omega(k_+) = \omega(k_-)$. In panels (c) and (d), condensation occurs at $k_{cp} = K$. In this case, particle-hole symmetry is broken, and we depict the dispersion of quasiparticles and quasiholes separately. In all panels, we have chosen $t = \rho = 1$.

Here, $\boldsymbol{\omega}(k) = [\omega_1(k), \omega_2(k), \omega_3(k)]^T$ represents lowest to highest eigenenergies at momentum k, respectively, for the Bogoliubov quasiparticles (k_+) and quasiholes (k_-). The lowest-energy band ω_1 should have zero energy at the condensation point which fixes the chemical potential μ [14,43].

In the BdG Hamiltonian, particle-hole symmetry (PHS) and TRS are defined as TRS: $H_B^*(k) = H_B(-k)$ and PHS: $\sigma_1 H_B^*(k)\sigma_1 = H_B(-k)$ [44,45]. We find that the symmetry properties of the BdG Hamiltonian depend on the choice of mean-field momentum: For $k_{cp} = \Gamma$, the complex-valued condensation parameters break TRS, while the diagonal blocks in the Bogoliubov Hamiltonian are the same; i.e., PHS is preserved. For $k_{cp} = K$, real-valued condensation parameters keep TRS intact, but the finite momentum of the condensate breaks PHS.

These symmetry properties have important consequences for the excitations whose spectra are plotted in Fig. 2 for the two different k_{cp}. For $k_{cp} = \Gamma$, PHS makes particle and hole spectra indistinguishable. They are plotted in Figs. 2(a) and 2(b) for two different values of V. For $k_{cp} = K$, particle and hole spectra are different, and plotted separately in Figs. 2(c) and 2(d), for the same choice of V as used in Fig. 2(a). The effect of TRS breaking is seen in Fig. 2(a) by the gap openings between all the bands in whole Brillouin zone, absent in Figs. 2(b)–2(d).

Broken TRS is also expected to have consequences for the topological properties of the collective modes; cf. Refs. [13,46–50]. Band curvature and Chern numbers are defined, respectively, as

$$B_m(k) = i\sum_{i,j}\epsilon_{ij}\langle\partial_i W(k)|\sigma_3|\partial_j W(k)\rangle_{mm}(\sigma_3)_{mm}, \quad (7)$$
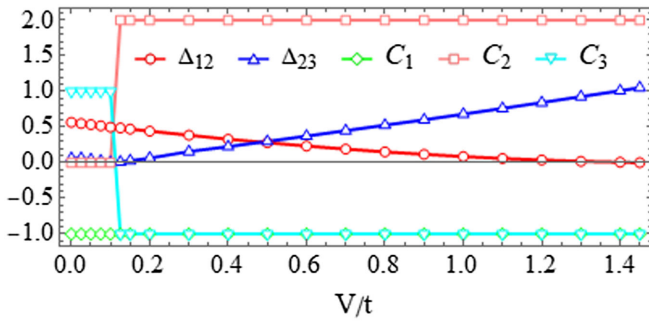
FIG. 3. The Chern number of Bogoliubov mode bands in addition to the energy gap between different bands for different values of the nearest-neighbor interaction V is plotted. The energy gap between the lowest (highest) and middle energy band, i.e., $\Delta_{12} = |\omega_1 - \omega_2|$ ($\Delta_{23} = |\omega_2 - \omega_3|$), is shown by a red circle (blue up triangle) line marker. The corresponding Chern numbers from lowest to highest energy band are specified as C_1, C_2, and C_3 with green diamond, pink square, and cyan down triangle line markers, respectively. Here, we supposed $U/t = 3$ and $\rho = 1$.

$$C_m = -\frac{1}{2\pi} \int_{BZ} d^2\mathbf{k} B_m(k). \tag{8}$$

Here, m stands for the Bogoliubov mode band index. We use the Fukui-Hatsugai-Suzuki method [51] to evaluate the Chern number for Bogoliubov excitation bands, making use of Eq. (8). Interestingly, as shown in Fig. 3, the condensate in Γ is not only topologically nontrivial, but also changes its topology upon tuning V. At very small V, the central band is topologically trivial, while bands 1 and 3 have Chern numbers -1 and 1. At $V/t \approx 0.11$, the gap Δ_{23} between the second and third bands touches zero, and then beyond this value for any $V/t \gtrsim 0.11$ all bands become topologically nontrivial: Bands 1 and 3 both acquire Chern number -1, whereas the central band exhibits a higher Chern number of value 2. This topology persists up to $V = U/2$, where the gap closing Δ_{12} between bands 1 and 2 yields another topological phase transition. However, as mentioned earlier, at this value also a structural change of the mean-field occurs.

Bulk-boundary correspondence.—The nontrivial topology of the Bogoliubov bands manifests itself also through chiral edge states. To study them, we apply a slab structure bounded along the y axis and composed of A, B sublattices at the two ends. We exploit translational invariance along the x axis and consider $N_y = 62$ sites along y. Details of the calculation for the bounded slab structure are provided in Supplemental Material [35]. Our main results are shown in Fig. 4, for $V = 0$ in the panels on the left and for $V/t = 0.6$ in the panels on the right. Within the gaps of the bulk Hamiltonian [plotted in Figs. 4(a) and 4(b)], the slab structure exhibits one in-gap mode [see spectra shown in Figs. 4(c) and 4(d)], which by their wave functions [plotted in Supplemental Material [35], panels (c) and (d)] as well as
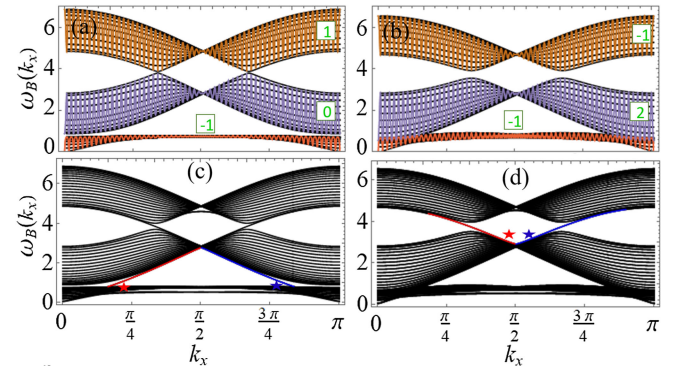

FIG. 4. Bulk dispersion relation of Bogoliubov quasiparticles above the Γ condensate, in panels (a) and (b). Dispersion relation of Bogoliubov quasiparticles above the Γ condensate, obtained from the bulk Hamiltonian in panels (a) and (b) and for the slab Hamiltonian in panels (c) and (d). The panels on the left (a),(c) are for $V = 0$ and on the right are for $V/t = 0.6$, while in all panels $U/t = 3$ is assumed. In the bulk Hamiltonian, all bands in different colors are energetically separated from each other, and Chern numbers are well defined (given in the boxes), although between the first and second bands in (b) the indirect band gap becomes zero. Noting the opposite group velocities of red and blue edge states, seen from the dispersion in (c) or (d), we interpret the pair as one chiral mode. Note that the chirality of the mode analyzed in the left panel is opposite to the chirality of the mode analyzed in the right panel. The chirality change is due to the topological transition at finite V, rendering the Chern number of the central band to 2 in the right panels.

by the condensate profile in the slab geometry [plotted in Supplemental Material [35], panels (a) and (b)] can be identified as localized edge states. The pair of blue and red states, at opposite edges and with opposite group velocities, can be interpreted as one chiral edge mode. In the figure, we have restricted our illustration to the edge states in the larger gaps, which exhibit sharper localization properties, but we note that both gaps in Fig. 4(c) exhibit an edge mode with the same chirality. This agrees with the trivial Chern number of the central band at $V = 0$, which from the bulk-boundary correspondence is not expected to produce any change in the edge states. On the other hand, in Fig. 4(d), the chirality of the mode in the second gap is opposite to the chirality of the mode in the first gap. The chirality change is expected due to the Chern number of the central band now being 2. Thus, the topology of the Bogoliubov quasiparticles is reflected by the chirality of the edge state, as expected from the bulk-boundary correspondence principle [13,52,53].

Discussion.—We have shown that nontrivial topological Bogoliubov excitation modes occur from the Γ-point condensate due to broken TRS in the corresponding BdG Hamiltonian but not from the K-point condensate. This is rather curious, since condensation in the Γ point is quite usual. Hence, the question arises whether the flatness of the band is required. We address this question by moving

the flat band from the lowest to the highest energy band by means of substituting $t \rightarrow -t$ in Eq. (1). The lowest-energy band then has a minimum energy at Γ. For $U \geq V$, we find uniform condensation [$d_\Gamma^\circ = (1, 1, 1)/\sqrt{3}$], whereas non-uniform condensation appears for $V > U$. Independent of the interaction parameters, both PHS and TRS are preserved in the BdG Hamiltonian, and the Bogoliubov excitations are topologically trivial. We conclude that the flatness of the lowest band is crucial to obtain the topological condensate.

However, as already found in Ref. [12], in the case of a flat lowest band, quantum fluctuations favor condensation in the K point which lacks the interesting topological behavior. How then can we have a system with a stable topologically nontrivial Γ-point condensate? Fortunately, there is a relatively simple mechanism which can act in favor of the Γ-point condensate: It has been shown in Ref. [34] that anisotropic hopping parameters in the kagome lattice can give rise to a substantially flat band with a controllable gap closing in the noninteracting Hamiltonian. Through this procedure, the number of condensation points can be reduced to one, at different high-symmetry points (Γ, K, M), depending on the choice of parameters. This then allows us to obtain a Γ-point condensate from the lowest flat band which is robust against quantum fluctuations and which has the same topologically nontrivial behavior reported above; see Supplemental Material [35]. Moreover, the construction allows us to remove the band-touching point and separate the flat band from the other bands on the single-particle level.

Experimental possibilities.—Our proposal here is experimentally feasible to realize with ultracold bosonic dysprosium atoms (or Rydberg atoms) in an optical lattice. The contact interaction for such an atomic species is already present. Importantly, they also possess a large magnetic dipole moment of $\sim 10\,\mu B$ which makes such atoms interact through dipole-dipole repulsion. So, tailoring a noninteracting lattice with shorter periodicity is necessary to have a generous value of nearest-neighbor interactions. In fact, tuning into different topological phases of the excitations becomes possible upon varying the lattice periodicity (or the Rydberg blockade radius) in such a system. The underlying noninteracting lattice itself can be generated by overlaying two commensurate triangular optical lattices with different wavelengths, as realized in Ref. [54]. The last ingredient necessary is a positive value of tunneling which can originate from a synthetic gauge flux as can be realized via circular lattice shaking [55]. The measurements of the topological edge states of the exotic excitation spectrum can then be carried out using two-photon-stimulated Raman transitions [56,57] which can load a macroscopic number of bosons from the condensate directly into the topological edge states. A time-of-flight measurement would then confirm the presence of vortices corresponding to the chiral topological modes.

[1] M. Z. Hasan and C. L. Kane, Colloquium: Topological insulators, Rev. Mod. Phys. **82**, 3045 (2010).

[2] X.-L. Qi and S.-C. Zhang, Topological insulators and superconductors, Rev. Mod. Phys. **83**, 1057 (2011).

[3] K. von Klitzing, The quantized Hall effect, Rev. Mod. Phys. **58**, 519 (1986).

[4] C. Nayak, S. H. Simon, A. Stern, M. Freedman, and S. Das Sarma, Non-Abelian anyons and topological quantum computation, Rev. Mod. Phys. **80**, 1083 (2008).

[5] M. Aidelsburger, M. Lohse, C. Schweizer, M. Atala, J. T. Barreiro, S. Nascimbene, N. R. Cooper, I. Bloch, and N. Goldman, Measuring the Chern number of Hofstadter bands with ultracold bosonic atoms, Nat. Phys. **11**, 162 (2015).

[6] B. Mukherjee, A. Shaffer, P. B. Patel, Z. Yan, C. C. Wilson, V. Crépel, R. J. Fletcher, and M. Zwierlein, Crystallization of bosonic quantum Hall states in a rotating quantum gas, Nature (London) **601**, 58 (2022).

[7] M. Di Liberto, A. Hemmerich, and C. Morais Smith, Topological Varma superfluid in optical lattices, Phys. Rev. Lett. **117**, 163001 (2016).

[8] J. Wang, W. Zheng, and Y. Deng, Pseudo-time-reversal-symmetry-protected topological Bogoliubov excitations of Bose-Einstein condensates in optical lattices, Phys. Rev. A **102**, 043323 (2020).

[9] X.-Q. Wang, G.-Q. Luo, J.-Y. Liu, W. V. Liu, A. Hemmerich, and Z.-F. Xu, Evidence for an atomic chiral superfluid with topological excitations, Nature (London) **596**, 227 (2021).

[10] Y. Cao, V. Fatemi, A. Demir, S. Fang, S. L. Tomarken, J. Y. Luo, J. D. Sanchez-Yamagishi, K. Watanabe, T. Taniguchi, E. Kaxiras, R. C. Ashoori, and P. Jarillo-Herrero, Correlated insulator behaviour at half-filling in magic-angle graphene superlattices, Nature (London) **556**, 80 (2018).

[11] D. Leykam, A. Andreanov, and S. Flach, Artificial flat band systems: From lattice models to experiments, Adv. Phys. **3**, 1473052 (2018).

[12] Y.-Z. You, Z. Chen, X.-Q. Sun, and H. Zhai, Superfluidity of bosons in kagome lattices with frustration, Phys. Rev. Lett. **109**, 265302 (2012).

[13] S. Furukawa and M. Ueda, Excitation band topology and edge matter waves in Bose–Einstein condensates in optical lattices, New J. Phys. **17**, 115014 (2015).

[14] A. Julku, G. M. Bruun, and P. Törmä, Excitations of a Bose-Einstein condensate and the quantum geometry of a flat band, Phys. Rev. B **104**, 144507 (2021).

[15] A. Julku, G. M. Bruun, and P. Törmä, Quantum geometry and flat band Bose-Einstein condensation, Phys. Rev. Lett. **127**, 170404 (2021).

[16] J.-S. Pan, W. Zhang, W. Yi, and G.-C. Guo, Bose-Einstein condensate in an optical lattice with Raman-assisted two-dimensional spin-orbit coupling, Phys. Rev. A **94**, 043619 (2016).

[17] J. Villain, R. Bidaux, J.-P. Carton, and R. Conte, Order as an effect of disorder, J. Phys. (Les Ulis, Fr.) **41**, 1263 (1980).

[18] R. Barnett, S. Powell, T. Grass, M. Lewenstein, and S. Das Sarma, Order by disorder in spin-orbit-coupled Bose-Einstein condensates, Phys. Rev. A **85**, 023615 (2012).

[19] G.-B. Jo, J. Guzman, C. K. Thomas, P. Hosur, A. Vishwanath, and D. M. Stamper-Kurn, Ultracold atoms in a tunable optical kagome lattice, Phys. Rev. Lett. **108**, 045305 (2012).

[20] J. Struck, C. Ölschläger, R. L. Targat, P. Soltan-Panahi, A. Eckardt, M. Lewenstein, P. Windpassinger, and K. Sengstock, Quantum simulation of frustrated classical magnetism in triangular optical lattices, Science **333**, 996 (2011).

[21] A. Petrescu, A. A. Houck, and K. Le Hur, Anomalous Hall effects of light and chiral edge modes on the kagomé lattice, Phys. Rev. A **86**, 053804 (2012).

[22] R. Chisnell, J. S. Helton, D. E. Freedman, D. K. Singh, R. I. Bewley, D. G. Nocera, and Y. S. Lee, Topological magnon bands in a kagome lattice ferromagnet, Phys. Rev. Lett. **115**, 147201 (2015).

[23] M. Li, D. Zhirihin, M. Gorlach, X. Ni, D. Filonov, A. Slobozhanyuk, A. Alù, and A. B. Khanikaev, Higher-order topological states in photonic kagome crystals with long-range interactions, Nat. Photonics **14**, 89 (2020).

[24] I. Titvinidze, J. Legendre, K. Le Hur, and W. Hofstetter, Hubbard model on the kagome lattice with time-reversal invariant flux and spin-orbit coupling, Phys. Rev. B **105**, 235102 (2022).

[25] Y.-J. Lin, R. L. Compton, K. Jiménez-García, J. V. Porto, and I. B. Spielman, Synthetic magnetic fields for ultracold neutral atoms, Nature (London) **462**, 628 (2009).

[26] M. Lewenstein, A. Sanpera, V. Ahufinger, B. Damski, A. Sen(De), and U. Sen, Ultracold atomic gases in optical lattices: Mimicking condensed matter physics and beyond, Adv. Phys. **56**, 243 (2007).

[27] J. Dalibard, F. Gerbier, G. Juzeliūnas, and P. Öhberg, Colloquium: Artificial gauge potentials for neutral atoms, Rev. Mod. Phys. **83**, 1523 (2011).

[28] M. Lewenstein, A. Sanpera, and V. Ahufinger, *Ultracold Atoms in Optical Lattices: Simulating Quantum Many-Body Systems* (Oxford University Press, New York, 2012).

[29] L. Lu, J. D. Joannopoulos, and M. Soljačić, Topological photonics, Nat. Photonics **8**, 821 (2014).

[30] N. Goldman, J. C. Budich, and P. Zoller, Topological quantum matter with ultracold gases in optical lattices, Nat. Phys. **12**, 639 (2016).

[31] T. Ozawa, H. M. Price, A. Amo, N. Goldman, M. Hafezi, L. Lu, M. C. Rechtsman, D. Schuster, J. Simon, O. Zilberberg, and I. Carusotto, Topological photonics, Rev. Mod. Phys. **91**, 015006 (2019).

[32] N. R. Cooper, J. Dalibard, and I. B. Spielman, Topological bands for ultracold atoms, Rev. Mod. Phys. **91**, 015005 (2019).

[33] J. Ruostekoski, Optical kagome lattice for ultracold atoms with nearest neighbor interactions, Phys. Rev. Lett. **103**, 080406 (2009).

[34] T. Bilitewski and R. Moessner, Disordered flat bands on the kagome lattice, Phys. Rev. B **98**, 235109 (2018).

[35] See Supplemental Material at http://link.aps.org/supplemental/10.1103/PhysRevLett.131.226601 for more mathematical and numerical simulation details which includes Refs. [36–41].

[36] A. Griffin, Conserving and gapless approximations for an inhomogeneous Bose gas at finite temperatures, Phys. Rev. B **53**, 9341 (1996).

[37] K. Suthar, A. Roy, and D. Angom, Fluctuation-driven topological transition of binary condensates in optical lattices, Phys. Rev. A **91**, 043615 (2015).

[38] N. Goldman, Mott-insulator transition for ultracold fermions in two-dimensional optical lattices, Phys. Rev. A **77**, 053406 (2008).

[39] M. Fishman, S. R. White, and E. M. Stoudenmire, The ITensor Software Library for Tensor Network Calculations, SciPost Phys. Codebases 4 (2022).

[40] P. Weinberg and M. Bukov, QuSpin: A PYTHON package for dynamics and exact diagonalisation of quantum many body systems part I: Spin chains, SciPost Phys. **2**, 003 (2017).

[41] D. van Oosten, P. van der Straten, and H. T. C. Stoof, Quantum phases in an optical lattice, Phys. Rev. A **63**, 053601 (2001).

[42] M.-w. Xiao, Theory of transformation for the diagonalization of quadratic Hamiltonians, arXiv:0908.0787.

[43] H. Shi and A. Griffin, Finite-temperature excitations in a dilute Bose-condensed gas, Phys. Rep. **304**, 1 (1998).

[44] T. Ohashi, S. Kobayashi, and Y. Kawaguchi, Generalized berry phase for a bosonic Bogoliubov system with exceptional points, Phys. Rev. A **101**, 013625 (2020).

[45] K. Yokomizo and S. Murakami, Non-Bloch band theory in bosonic Bogoliubov–de Gennes systems, Phys. Rev. B **103**, 165123 (2021).

[46] G. Engelhardt and T. Brandes, Topological Bogoliubov excitations in inversion-symmetric systems of interacting bosons, Phys. Rev. A **91**, 053621 (2015).

[47] G.-H. Huang, G.-Q. Luo, Z. Wu, and Z.-F. Xu, Interaction-induced topological Bogoliubov excitations in a spin-orbit-coupled Bose-Einstein condensate, Phys. Rev. A **103**, 043328 (2021).

[48] R. Shindou, R. Matsumoto, S. Murakami, and J. I. Ohe, Topological chiral magnonic edge mode in a magnonic crystal, Phys. Rev. B **87**, 174427 (2013).

[49] R. Shindou, J. I. Ohe, R. Matsumoto, S. Murakami, and E. Saitoh, Chiral spin-wave edge modes in dipolar magnetic thin films, Phys. Rev. B **87**, 174402 (2013).

[50] Y.-Q. Wang and X.-J. Liu, Dirac and topological phonons with spin-orbital entangled orders, arXiv:1710.02070.

[51] T. Fukui, Y. Hatsugai, and H. Suzuki, Chern numbers in discretized brillouin zone: Efficient method of computing (spin) Hall conductances, J. Phys. Soc. Jpn. **74**, 1674 (2005).

[52] Y. Hatsugai, Chern number and edge states in the integer quantum Hall effect, Phys. Rev. Lett. **71**, 3697 (1993).

[53] M. Z. Hasan and C. L. Kane, Colloquium: Topological insulators, Rev. Mod. Phys. **82**, 3045 (2010).

[54] G.-B. Jo, J. Guzman, C. K. Thomas, P. Hosur, A. Vishwanath, and D. M. Stamper-Kurn, Ultracold atoms in a tunable optical kagome lattice, Phys. Rev. Lett. **108**, 045305 (2012).

[55] G. Jotzu, M. Messer, R. Desbuquois, M. Lebrat, T. Uehlinger, D. Greif, and T. Esslinger, Experimental realization of the topological Haldane model with ultracold fermions, Nature (London) **515**, 237 (2014).

[56] M. F. Andersen, C. Ryu, P. Cladé, V. Natarajan, A. Vaziri, K. Helmerson, and W. D. Phillips, Quantized rotation of atoms from photons with orbital angular momentum, Phys. Rev. Lett. **97**, 170406 (2006).

[57] T. D. Stanescu, V. Galitski, J. Y. Vaishnav, C. W. Clark, and S. Das Sarma, Topological insulators and metals in atomic optical lattices, Phys. Rev. A **79**, 053639 (2009).